Quantum-interference-controlled resonance profiles from lasing without inversion to photodetection

Konstantin E. Dorfman,[1,*] Pankaj K. Jha,[1,†] and Sumanta Das[2,‡]

[1]*Institute for Quantum Science and Engineering and Department of Physics and Astronomy, Texas A&M University, College Station, Texas 77843-4242, USA*

[2]*Zur Forstquelle 6, 69126 Heidelberg, Germany*

(Received 7 August 2011; published 2 November 2011; corrected 5 January 2012)

In this work we report a quantum interference mediated control of the resonance profiles in a generic three-level system and investigate its effect on key quantum interference (QI) phenomena. Namely in a three-level configuration with doublets in the ground or excited states, we show control over enhancement and suppression of the emission (absorption) profiles. This is achieved by manipulation of the strength of QI and the energy spacing of the doublets. We analyze the application of such QI-induced control of the resonance profile in the framework of two limiting cases of lasing without inversion and photodetection.

DOI: 10.1103/PhysRevA.84.053803 PACS number(s): 42.50.Gy, 42.50.Lc, 73.21.−b, 78.56.−a

I. INTRODUCTION

Study of quantum interference (QI) had led to the discovery of numerous fascinating phenomena in various types of systems ranging from atoms to biomolecules [1–3]. In atomic systems, for example, one of the earliest known effects of QI is the modification of the absorption profiles that comes about due to interference among the bound-bound and bound-continuum transitions, a phenomenon now called Fano interference [4]. Agarwal [5] later showed how QI among decay pathways can lead to generation of coherence and population trapping in a multilevel atomic configuration. A counterintuitive application of such *Agarwal-Fano QI* was discovered by Harris in the form of inversionless lasing (LWI) [6]. This nonenergy-conserving phenomena had thereof led to several theoretical investigations [7–9] and experimental demonstration [10–12]. Furthermore, during the past decade study of QI effects has been extended to tailored semiconductor nanostructures like quantum wells and dots due to coherent resonant tunneling owing to their potential applications in photodetection [13,14], lasing [15,16], quantum computing, and quantum circuitry [17,18].

In the seminal work of Scully [19] it was shown that coherence induced by an external source can break the detailed balance between emission and absorption and enhance, in principle, the quantum efficiency of a photovoltaic cell. Reference [19] demonstrated the role of quantum coherence in a simple way. In a recent work we showed that coherence induced by QI can enhance the power of the Photocell and Laser Quantum Heat Engines [20,21] following the earlier work on the Photo-Carnot Engine enhanced by quantum coherence [22]. The main idea is that the quantum coherence induced by either an external drive or QI among the decay paths alters the detailed balance between emission and absorption and can enhance the efficiency of the system compared to that without quantum coherence. In the case of photovoltaic cells, quantum coherence leads to suppression of radiative recombination [19] or enhancement of absorption [21] and thus, an increase in the efficiency. Furthermore, the results of Ref. [19] have initiated debates about the principle issues. In his article, Kirk [23] attempts to investigate the limits of Ref. [19] and, in particular, argues that Fano interference does not break detailed balance of the photocell. Note that noise-induced coherence via Fano interference was later shown to indeed enhance the balance breaking in photovoltaics where it leads to an increase in power [20,21,24,25].

These investigations have hence generated renewed interest in the fundamental question of noise-induced interference effects on the emission and absorption profile of an atom or atom-like system (excitons in quantum wells or dots) [26]. As such, we in this paper undertake a thorough theoretical investigation of the vacuum-induced interference effects on the resonance line profiles of a three-level system with doublets in ground (excited)-state configuration (see Fig. 1). Our analysis is quite general and applies to atoms, molecules, as well as quantum wells and dots. We study the time profile of absorption and emission probabilities and derive its close form expression in the steady-state regime. In the present work we use a simple probability amplitude method to calculate the resonance profiles since the states involved in calculation have a zero-photon occupation number. The latter is equivalent to the density matrix formalism usually used in this type of problem [20,21].

The probabilities of emission and absorption are found to have strong functional dependence on the energy spacing between the doublets (2Δ) and interaction strength p. In the case of the atomic system, p is governed by a mutual orientation of dipole moments. In semiconductor systems p has a meaning of the phase shift acquired by the wave function between two interfering pathways. This thus provides us with two different parameters by which we can regulate the QI in the system. For example, we show that depending on the choice of energy spacing between the doublets compared to the spontaneous decay rate we can use destructive interference to achieve either LWI by enhancing the emission or photodetectors and interferometers by reducing emission and enhancing absorption. Moreover, depending on p we can manipulate the interference type from destructive to constructive which can significantly alter the resonance profiles (see Fig. 3).

*dorfman@physics.tamu.edu

†pkjha@physics.tamu.edu

‡Currently at Max-Planck Institut für Kernphysik, Heidelberg, Germany.

The outline of the paper is as follows. In Sec. II, we present our theoretical model of the three-level system with the doublet in the ground state and calculate the expression for the probability of emission P_{emiss} and absorption P_{abs} in the long time limit $t \gg \gamma^{-1}, \Gamma^{-1}$. Furthermore, we also give results for emission and absorption probabilities for a three-level configuration with the upper state doublet. In Sec. III, the functional form of the ratio $P_{\text{emiss}}/P_{\text{abs}}$ is presented to quantify its dependence on the dipole alignment parameter p, energy spacing (2Δ), and the radiative decay rates Γ, γ. We discuss our results and propose a potential application of our model to enhancement of emission in LWI configuration, enhancement of absorption for photodetectors, and observation of QED results on quantum beats in the semiclassical regime. Finally in Sec. IV we conclude by summarizing our findings.

II. THEORETICAL MODEL

In order to investigate the effect of QI on the emission and absorption profile of an atomic, molecular, or semiconductor system we consider a three-level configuration with a ground-state doublet $|v_{1,2}\rangle$ and excited state $|c\rangle$ [see Fig. 1(a)]. The three-level system is excited by the coherent field with the central frequency ν so that the energies of state $|v_{1,2}\rangle$ are related to $|c\rangle$ as $\nu \pm \Delta$, where Δ is half of the energy spacing between the ground-state doublet. The ground-state doublet $|v_{1,2}\rangle$ decays to the reservoir state R_v with the rate $2\gamma_{1,2}$, respectively, and the excited state decays to the reservoir state R_c with the decay rate 2Γ. Furthermore, states $|v_{1,2}\rangle$ can represent either Zeeman sublevels in atoms, vibrational levels within the electronic band in molecules or intrasubband in semiconductors. Since the typical relaxation rate of electronic (intersubband) transition is much smaller than that of vibrational (intrasubband), we neglect the direct decay process between level $|c\rangle$ and $|v_{1,2}\rangle$. Note that the decay of ground-state doublets $|v_{1,2}\rangle$ to the same state $|R_v\rangle$ leads to a vacuum-induced coherence among them. The physics of this coherence is attributed to the *Agarwal-Fano QI* of the transition amplitudes among the decay pathways. Note that the analysis presented below is valid for the system with the excited state doublet $|c_{1,2}\rangle$ and single ground state $|v\rangle$ [as per Fig. 1(b); see discussion]. We will show later that such QI plays a major role in the line profiles of an atomic system [6,27]. The time-dependent amplitudes of the states $|v_{1,2}\rangle$ and $|c\rangle$ essentially exhibits the effect of coherence on the dynamics of the system. The probability amplitude method can be applied in the present system since states $|v_{1,2}\rangle$ and $|c\rangle$ have a zero-photon occupation number. Solving the time-dependent Schrödinger equation, the dynamical evolution of the probability amplitudes $v_{1,2}$ and c of finding a system in corresponding states $|v_{1,2}\rangle$ and $|c\rangle$ (i.e., states with zero photons) in Weisskopf-Wigner approximation is given by

$$\dot{v}_2(t) = -(\gamma_2 + i\Delta)v_2(t) - p\sqrt{\gamma_1\gamma_2}v_1(t) - i\Omega_2 c(t), \quad (1)$$

$$\dot{v}_1(t) = -(\gamma_1 - i\Delta)v_1(t) - p\sqrt{\gamma_1\gamma_2}v_2(t) - i\Omega_1 c(t), \quad (2)$$

$$\dot{c}(t) = -i\Omega_2 v_2(t) - i\Omega_1 v_1(t) - \Gamma c(t), \quad (3)$$

where $\Omega_{1,2} = \wp_{1,2}\mathcal{E}_0/2\hbar$ and $\wp_{1,2}$ are the respective Rabi frequencies and dipole moments of the corresponding transitions $|v_{1,2}\rangle \leftrightarrow |c\rangle$ with $\mathcal{E}_0$ being the amplitude of the applied electric field. The term $p\sqrt{\gamma_1\gamma_2}$ arises due to QI of the decay pathways of the ground-state doublet. It is clearly seen from the above set of equations that this term for $p \neq 0$ couples the amplitudes of the states v_1 and v_2. Such a coupling is known as *Agarwal-Fano coupling* in the literature [28] and has several implications ranging from superradiance [29,30] and entanglement [30] to quantum solar cells [19–21]. The interference strength is typically determined in terms of the relative orientation of the dipole moments of the decay transitions and is given by coefficient p as

$$p = \frac{\vec{\wp}_{v_1 R_v} \cdot \vec{\wp}_{v_2 R_v}}{|\vec{\wp}_{v_1 R_v}||\vec{\wp}_{v_2 R_v}|}, \quad (4)$$

where $\vec{\wp}_{v_1 R_v}$ and $\vec{\wp}_{v_2 R_v}$ are the dipole moment corresponding to the transition $|v_1\rangle \leftrightarrow |R_v\rangle$ and $|v_2\rangle \leftrightarrow |R_v\rangle$, respectively, with $p = \pm 1$ exhibiting the maximal interference among the decay paths. Here $p = 1$ corresponds to the two dipole moment vectors parallel to each other on the other hand when they are antiparallel $p = -1$. Nonorthogonal dipole moments in optical transition have been generated using superposition of singlet and triplet states due to spin-orbit coupling in sodium dimers [31]. More generally, interference strength p is a phase shift acquired by wave function between initial and final states. Equations (1)–(3) can be written and solved in the dressed basis using the approach developed by Scully [32] as discussed in Appendix A for general p and in the presence of additional decay rates Γ, γ. The probability of emission P_{emiss} defined as a sum of population of the doublet $|v_1\rangle$, $|v_2\rangle$ and of the reservoir state $|R_v\rangle$ due to conservation of probability, can be written in terms of populations of states $|c\rangle$ and $|R_c\rangle$ as

$$P_{\text{emiss}}(\tau|c) = 1 - |c(\tau)|^2 - 2\tilde{\Gamma}\int_0^\tau |c(\tau')|^2 d\tau'. \quad (5)$$

In the long time limit, $\tau \gg 1, 1/\tilde{\Gamma}$ and assuming $\gamma_1 = \gamma_2 = \gamma$ for simplicity, the probability of emission defined in Eq. (5) (derived in Appendix B) yields

$$P_{\text{emiss}}(\infty|c) = \frac{(\tilde{\Gamma}+1)\left(\tilde{\Omega}_1^2 + \tilde{\Omega}_2^2\right) - 2p\tilde{\Omega}_1\tilde{\Omega}_2}{\tilde{\Gamma}[(\tilde{\Gamma}+1)^2 + \tilde{\Delta}^2 - p^2]}, \quad (6)$$

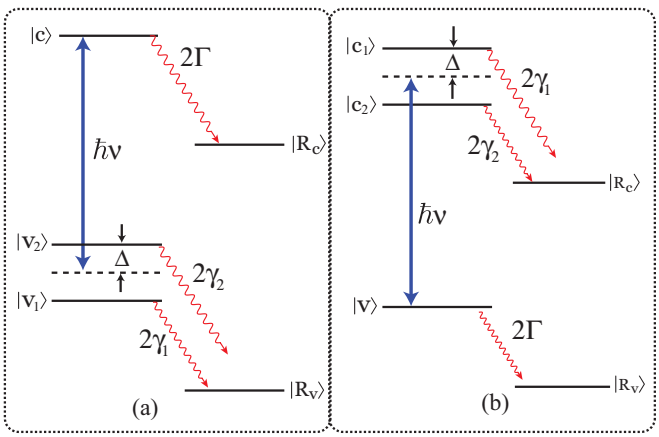

FIG. 1. (Color online) The scheme of the three-level system with the doublet in the ground state (a) and in the excited state (b). Radiative decay from the doublet states to the reservoir is 2γ while the excited (ground) state to the reservoir is 2Γ.

where the tilde signifies that all the parameters are now dimensionless as they are normalized by γ. The probability of absorption from level $|v_1\rangle$ can be evaluated in a similar manner. For the initial conditions $v_1(0) = 1$, $v_2(0) = 0$ and $c(0) = 0$ the probability of absorption $P_{\rm abs}$ is given by the sum of population on states $|c\rangle$ and $|R_c\rangle$:

$$P_{\rm abs}(\tau|v_1) = |c(\tau)|^2 + 2\tilde{\Gamma}\int_0^\tau |c(\tau')|^2 d\tau', \tag{7}$$

which yields the following expression in the long time limit, $\tau \gg 1, 1/\tilde{\Gamma}$ (see Appendix B):

$$P_{\rm abs}(\infty|v_1) = \frac{1}{\mathcal{D}}\{[2(1+\tilde{\Delta}^2)(1+\tilde{\Gamma}) - \tilde{\Gamma}p^2]\tilde{\Omega}_1^2 - 2(\tilde{\Gamma}+2)p\tilde{\Omega}_1\tilde{\Omega}_2 + (\tilde{\Gamma}+2)p^2\tilde{\Omega}_2^2\}, \tag{8}$$

where $\mathcal{D} = 2(1+\tilde{\Delta}^2 - p^2)[(\tilde{\Gamma}+1)^2 + \tilde{\Delta}^2 - p^2]$. The probability of absorption from level $|v_2\rangle$ can be derived in the same way as for the level $|v_1\rangle$ by interchanging $v_1 \leftrightarrow v_2$ in Eq. (7) and $\tilde{\Omega}_1 \leftrightarrow \tilde{\Omega}_2$ in Eq. (8). Comparison of Eq. (6) with Eq. (8) yields that probability of emission and absorption can vary substantially in the presence ($p \neq 0$) or absence ($p = 0$) of interference.

So far we have discussed a model with the doublet in the ground state. Let us now consider the doublet in the excited state [as shown in Fig. 1(b)]. In practice this configuration is commonly used in semiconductor systems like quantum wells and dots. The expression for the probability of emission and absorption in the case of the excited state doublet can be obtained as follows. If we start with $|c_1\rangle$, the probability of emission is given by

$$P_{\rm emiss}(\tau|c_1) = |v(\tau)|^2 + 2\tilde{\Gamma}\int_0^\tau |v(\tau')|^2 d\tau'. \tag{9}$$

Similarly, the probability of absorption from $|v\rangle$ yields

$$P_{\rm abs}(\tau|v) = 1 - |v(\tau)|^2 - 2\tilde{\Gamma}\int_0^\tau |v(\tau')|^2 d\tau'. \tag{10}$$

The expression for the emission and absorption probability can be calculated by following a procedure similar to that outlined in Appendix B for the ground-state doublet. In the long time limit $t \gg \gamma^{-1}, \Gamma^{-1}$, we find that the expression for emission and absorption probabilities obtained from Eqs. (9) and (10) reduces to Eqs. (8) and (6), respectively.

III. DISCUSSION

A. Applications to lasing without inversion and photodetectors

The model discussed in the previous section is relevant for the design of systems with a nonreciprocal relation between emission and absorption. For instance, suppressed absorption or/and enhanced emission in the laser systems allows for operating without population inversion. On the other hand enhanced absorption with suppressed emission can result in the photodetector or photovoltaic (solar) cell system with enhanced power output [20,21]. Both LWI and photodetector schemes can be realized in atomic molecular and semiconductor systems. In atoms Agarwal-Fano type QI can arise between decay channels from magnetic sublevels. In molecular systems on the other hand, decay pathways of different vibrational and rotational levels lead to asymmetric absorption and emission profiles due to interference. In the case of semiconductors, Agarwal-Fano interference comes about quite naturally in a system of two quantum wells or dots grown at nanometer separations [15,16]. The tunneling and Förster interactions among the wells and dots renormalizes the bare energies and bare states of the system thereby creating new eigenstates, which then reveals the interference in decay channels through tunneling to the same continuum [32,33]. Note that QI and coherence effects in semiconductors are strongly effected by the presence of the dephasing environment and hence experiments in these systems are carried out at very low temperatures (10 K). This thereby restricts their practical feasibility for various applications involving QI. However, recently a quantum dot photodetector enhanced by Fano-type interference assisted with a metallic hole array was reported operating at 77 K [14]. Hence in the near future realization of Fano-like QI effects in nanostructures and its various applications might be achievable even at room temperatures.

To put the above ideas into perspective, we discuss the functional dependence of the emission and absorption probabilities on the interference strength p and the level spacing Δ in the steady-state and transient regime. We show in Fig. 2 the steady-state behavior and temporal evolution of emission and absorption probabilities for different values of p and Δ. Figures in the upper panels [Figs. 2(a)–2(c)] correspond to large level spacing compared to spontaneous decay rate $\Delta \gg \gamma$ ($\tilde{\Delta} \gg 1$). The steady-state emission profile is seen to be strongly influenced by the strength of QI. It varies from its minimum at $p = 1$ to maximum at $p = -1$ [see Fig. 2(a)]. The enhancement in emission is found to be almost tenfold. However, for absorption the effect of interference is not significant as p varies from -1 to 1. Therefore, for $p = -1$ one can achieve the regime with the largest emission, which can be useful in inversionless lasing schemes. On the other hand at $p = 1$, as emission reaches its minimum, it is attractive in realization of photodetectors and photovoltaic devices. Note that in the semiconductor double quantum well system, control over p can be achieved by manipulating the width of the shallow well [16]. The time evolution of the resonance profiles shown in Figs. 2(b) and 2(c) exhibits oscillatory behavior in the emission and absorption probabilities. The period of oscillations is determined by the frequency $\sqrt{\Delta^2 - \gamma^2}$ and thus strongly depends on the level spacing. We see further that the oscillations get damped with time and the probabilities eventually reach the steady state.

For small level spacing $\Delta \ll \gamma$ ($\tilde{\Delta} \ll 1$), the situation becomes less trivial. In this case the behavior of emission and absorption profiles is depicted in the lower panel of Figs. 2(d)–2(f). In the steady state both the probabilities vary significantly with the interference strength p [see Fig. 2(d)]. We find that while absorption probability increases monotonically from $p = 1$ to $p = -1$, emission is seen to first increase until about $p = -0.5$ beyond which it rapidly decreases to reach the minimum value at $p = -1$. This is in sharp contrast to the behavior of the emission probability for large Δ. In the time-dependent profiles [Figs. 2(e) and 2(f)] we find that in comparison to the case of large splitting both emission and absorption probabilities show no oscillations and reach their

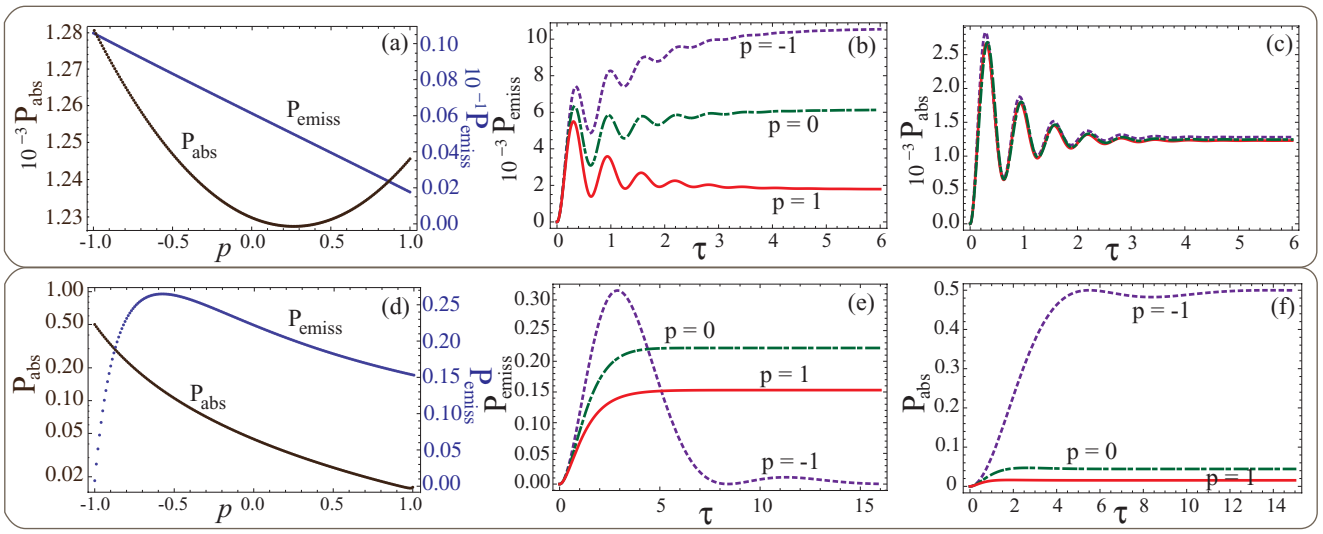

FIG. 2. (Color online) Steady state (a) and (d) and temporal evolution (b), (c), (e), and (f) of the emission and absorption probability for the three-level model with the doublet in the ground state. (a)and (d) Show the effect of the parameter "p" on the steady-state values of the probability of emission and absorption. (b) and (e) Show the temporal behavior of the probability of emission for three choices of "p." (c) and (f) Show the temporal behavior of the probability of absorption for the same choices of p as in (b) and (e). For numerical simulation we took $\Omega_1 = \Omega_2 = 0.3\gamma$, $\Gamma = 0.4\gamma$, and $\Delta = 10\gamma$ for (a)–(c) and $\Delta = 0.01\gamma$ for (d)–(f).

steady-state values that depend strongly on the interference strength. Furthermore, an interesting case arise at $p = -1$ where emission profile first reaches its maximum and then drops down to the steady state that has the smallest value compared to other $p \neq -1$. In the same time absorption profile at $p = -1$ reaches its maximum value at steady state. Note that in contrast to that, for large splitting at $p = -1$ emission has its maximum [see Fig. 2(b)]. Therefore, not only interference strength determines the emission and absorption profile, but the level spacing itself has a strong impact. Namely, for a fixed value of p, for example, $p = -1$, large level spacing Δ yields the strongest emission [see Fig. 2(b)] which is in favor of the lasing process. In the same time for small level spacing the emission is strongly suppressed while absorption reaches its maximum [see Figs. 2(e) and 2(f)], which is the perfect situation for photodetection and photocell operation. Furthermore, it is worth noting that despite the asymmetry between curves for $p = \pm 1$ in Fig. 2, results for $p = 1$ can be derived from the $p = -1$ case by changing the sign of the Rabi frequency, for instance, $\Omega_1 \to -\Omega_1$.

To study further the effects of p and Δ and to understand the special case of antiparallel alignment $p = -1$ consider the ratio of emission and absorption given by Eqs. (6) and (8):

$$\frac{P_{\text{emiss}}}{P_{\text{abs}}} = \frac{2(1+\tilde{\Gamma}-p)(1+\tilde{\Delta}^2-p^2)}{\tilde{\Gamma}[\tilde{\Delta}^2(1+\tilde{\Gamma})+\tilde{\Gamma}(1-p)+(1-p)^2]}, \quad (11)$$

where for simplicity we assume $\Omega_1 = \Omega_2$. Figure 3 shows the ratio in Eq. (11) as a function of interference strength p for the case of small and large level spacing. If the spacing is small, $\Delta \ll \gamma$, then the ratio in Eq. (11) monotonically increasing from $p = -1$ to $p = 1$, while for large spacing $\Delta \gg \gamma$, the behavior is essentially the opposite (i.e., it is a monotonically decreasing function as we mention above). Furthermore, in the limit of weak field $\Omega_1 = \Omega_2 = \Omega \ll 1$ Eq. (11) yields for $p = 0, 1$ a result that is independent of Δ. Namely for no interference (i.e., $p = 0$), Eq. (11) yields $2/\tilde{\Gamma}$, while for parallel alignment $p = 1$ it yields $2/(1+\tilde{\Gamma})$. On the other hand the case of antiparallel alignment ($p = -1$) is special. In particular, for small spacing $\Delta \ll \Gamma \ll \gamma$ Eq. (11) gives $\tilde{\Delta}^2/\tilde{\Gamma} \ll 1$, while for $\Delta \gg \gamma$ and $\Gamma \ll \gamma$ the result is $4/\tilde{\Gamma} \gg 1$. Therefore, the present analysis not only confirms that destructive interference can alter the detailed balance but also exhibits that by controlling two parameters. Namely by adjusting the interference strength p and energy spacing Δ, one can regulate the ratio between emission and absorption probabilities in the system. This possible manipulation of p and Δ hence also suggest that in the same system with two lower (upper) levels one can induce either suppression of emission [20,21] or absorption [15,16], respectively. The later choice governed by level spacing Δ can be also controlled externally either by adjusting the current through the junction, or by manipulating the magnetic field in hyperfine splitting

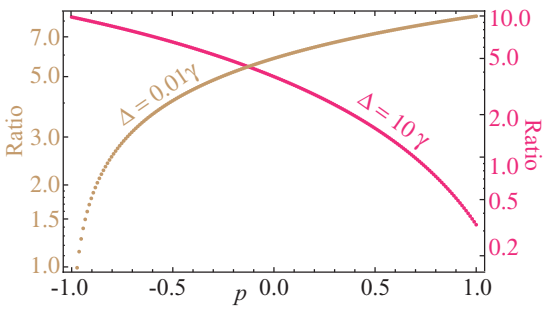

FIG. 3. (Color online) Ratio of the probability of emission to absorption for two combinations of coupling Δ as a function of the parameter p. For numerical simulation we took $\Omega_1 = \Omega_2 = 0.3\gamma$, $\Gamma = 0.4\gamma$.

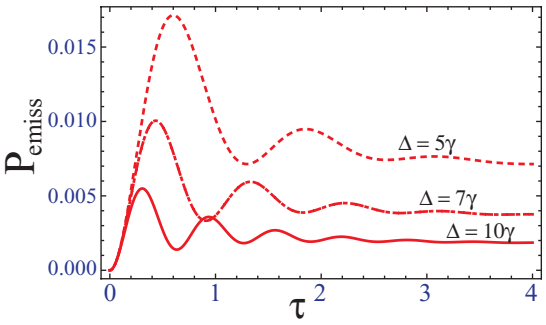

FIG. 4. (Color online) Probability of emission in the three-level model lower doublet for different choices of Δ. For numerical simulation we took $\Omega_1 = \Omega_2 = 0.3\gamma$, $\Gamma = 0.4\gamma, \gamma = 1, \tau = \gamma t$, $p = 1$.

[34,35]. In Fig. 4. we have plotted the effect of Δ on the temporal evolution of the probability of emission. The results show that the oscillations in the probability varies with the increase of Δ. Furthermore, for fixed Δ and γ the number of oscillations is governed by rate Γ since probability decays as $\exp(-\Gamma t)$. For interference strength p, control can be achieved by a tailored variation of the quantum well widths [16]. Summarizing the proposed scheme with lower doublet can be applied to the system that requires emission (absorption) suppression or enhancement and thus is very attractive for both: light emitting devices, such as LWI and light absorbing photodetector systems.

B. Quantum beats in semiclassical picture

Besides a broad range of applications, interference effects and in particular its sensitivity to the level spacing discussed in the present work are related to fundamental question about the applicability of semiclassical theory in quantum problems. Semiclassical description (SCT) can predict self-consistent and physically acceptable behavior of many physical systems and explain almost all quantum phenomena. However, it is not always correct. For instance, the phenomena of quantum beats has a substantially different result if considered in the

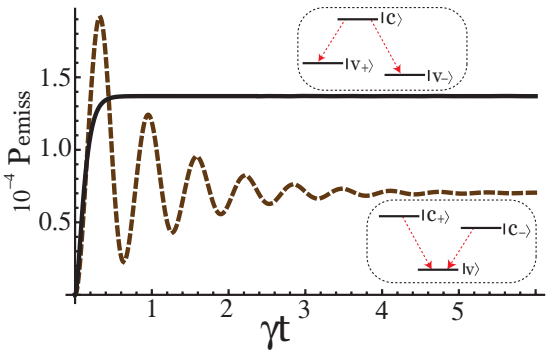

FIG. 5. (Color online) Probability of emission P_{emis} as a function of dimensionless time τ for three-level system with doublet in excited state (dashed line) and for three-level system with doublet in ground state (solid line) calculated numerically according to Eqs. (5) and (7) based on the solution of Eqs. (1)–(3). For numerical simulations we took $\Omega_1 = 0.1\gamma, \Omega_2 = 0.08\gamma, \Gamma = 10\gamma, \Delta = 0.1\gamma$.

framework of quantum electrodynamics (QED) [1], namely, for different configurations of three-level systems: for instance, V and Λ schemes (see Fig. 5) that are initially prepared in a coherent superposition of all three states SCT description predicts the existence of quantum beats for both schemes, whereas QED theory predicts no quantum beats in the case of the Λ scheme. The explanation of the phenomenon is quite straightforward and based on quantum theory of measurements. In the case of the V scheme the coherently excited atom decays to the same final state $|v\rangle$ starting from $|c_+\rangle$ and $|c_-\rangle$ and one cannot determine which decay channel was used. Therefore this interference that is similar to the double-slit problem leads to the existence of quantum beats. However, in the case of the Λ scheme that has also two decay channels, $|c\rangle \to |v_+\rangle$ and $|c\rangle \to |v_-\rangle$, after a long time the observation of the atom's final state ($|v_+\rangle$ or $v_-\rangle$) will determine which decay channel was used. In this case we do not expect quantum beats. Three-level systems with the doublet in the ground state or excited state is in a way similar to the Λ and V types of atom, respectively. Therefore we can also study the quantum beat's effect in those systems. Note that in the model of Fig. 1 we have additional radiative decays of states, which guarantees that the system can reach a steady state within a finite amount of time. Figure 5 illustrates that in the case of the doublet in the excited state (V scheme) with large spacing between levels $|c_+\rangle$ and $|c_-\rangle$ $\tilde{\Delta} \gg 1$, the probability of emission oscillates as a function of time and reaches the steady state at the time scale determined by radiative decay $1/\tilde{\Gamma} \gg 1$. However, for the case of the doublet in the ground state (Λ scheme) with small spacing $\tilde{\Delta} \ll 1$, the probability of emission does not process any quantum beats and smoothly reaches the steady state. Therefore, the phenomenon of Fano interference has the potential to resolve the fundamental question about the applicability of the semiclassical description to the problem of quantum beats.

IV. CONCLUSION

To conclude, in this paper we investigated the effect of vacuum-induced QI on the emission (absorption) profile of a three-level system with a doublet in the ground or excited state [see Fig. 1(a)]. We show that QI can enhance the balance breaking between emission and absorption. We use the probability amplitude method, since the states involved in calculation have a zero-photon occupation number. Furthermore, our findings are in full agreement with the results obtained by density matrix formalism. We observed that the interference strength p governed by the phase shift between the decay pathways play a crucial role on the emission(absorption) dynamics of the system. For the closely spaced doublet ($\Delta \ll \gamma$), for which the vacuum-induced QI becomes important, the behavior of the emission (absorption) profile of our model appears counterintuitive. For $p \sim -1$, the ratio of probability of emission to probability of absorption is very small, a condition favorable for applications like photovoltaics. On the other hand for $p \sim 1$, the ratio is large thus favorable for amplification without population inversion in steady state (see Figs. 2(b) and 2(e)]. In addition to these applications we found that Agarwal-Fano QI can also predict the occurrence of fundamental phenomena like quantum beats

in the semiclassical framework, which fully agrees with the QED description.

ACKNOWLEDGMENTS

We thank Anatoly Svidzinsky and Dong Sun for useful and stimulating discussion and acknowledge support from the Office of Naval Research, Robert A. Welch Foundation (Award No. A-1261). P.K.J. also acknowledges Herman F. Heep and Minnie Belle Heep, Texas A&M University Endowed Fund held and administered by the Texas A&M Foundation.

APPENDIX A: THE SCULLY DRESSED STATE ANALYSIS

We start with evolution of amplitudes in Eqs. (1)–(3) for $\gamma_1 = \gamma_2 = \gamma$,

$$\dot{v}_2 = -(\gamma + i\Delta)v_2 - p\gamma v_1 - i\Omega_2 c, \tag{A1}$$

$$\dot{v}_1 = -(\gamma - i\Delta)v_1 - p\gamma v_2 - i\Omega_1 c, \tag{A2}$$

$$\dot{c} = -i\Omega_2 v_2 - i\Omega_1 v_1 - \Gamma c, \tag{A3}$$

Writing Eqs. (A1)–(A3) in matrix form, we obtain

$$\frac{d}{d\tau}\begin{pmatrix} v_2 \\ v_1 \\ c \end{pmatrix} = -\Gamma_0 \begin{pmatrix} v_2 \\ v_1 \\ c \end{pmatrix} - iV \begin{pmatrix} v_2 \\ v_1 \\ c \end{pmatrix}, \tag{A4}$$

where $\tau = \gamma t$, and the Fano decay matrix is defined by

$$\Gamma_0 = \begin{pmatrix} 1 + i\tilde{\Delta} & p & 0 \\ p & 1 - i\tilde{\Delta} & 0 \\ 0 & 0 & \Gamma \end{pmatrix}, \tag{A5}$$

and probe-field interaction is given by

$$V = \begin{pmatrix} 0 & 0 & \tilde{\Omega}_2 \\ 0 & 0 & \tilde{\Omega}_1 \\ \tilde{\Omega}_2 & \tilde{\Omega}_1 & 0 \end{pmatrix}, \tag{A6}$$

with $\tilde{\Delta} = \frac{\Delta}{\gamma}$ and $\tilde{\Omega}_{1,2} = \frac{\Omega_{1,2}}{\gamma}$.

It is intuitive to introduce a basis in which the Fano coupling is transformed away. We proceed from the bare basis via the U, U^{-1} matrices of diagonalization.

$$U^{-1} = \frac{1}{\sqrt{2}p}\begin{pmatrix} p & p & 0 \\ x - i\tilde{\Delta} & -x - i\tilde{\Delta} & 0 \\ 0 & 0 & \sqrt{2}p \end{pmatrix}, \tag{A7}$$

$$U = \frac{1}{\sqrt{2}x}\begin{pmatrix} x + i\tilde{\Delta} & p & 0 \\ x - i\tilde{\Delta} & -p & 0 \\ 0 & 0 & \sqrt{2}x \end{pmatrix}. \tag{A8}$$

Here $x = \sqrt{p^2 - \tilde{\Delta}^2}$, so that the transformed state vector is defined by

$$U\begin{pmatrix} v_2 \\ v_1 \\ c \end{pmatrix} = \begin{pmatrix} V_+ \\ V_- \\ C \end{pmatrix}, \tag{A9}$$

which implies

$$V_\pm = \frac{(x \pm i\tilde{\Delta})v_2 \pm pv_1}{\sqrt{2}x}, \tag{A10}$$

and thus,

$$\begin{pmatrix} \dot{V}_+ \\ \dot{V}_- \\ \dot{C} \end{pmatrix} = -\Gamma_t \begin{pmatrix} V_+ \\ V_- \\ C \end{pmatrix} - iV_t \begin{pmatrix} V_+ \\ V_- \\ C \end{pmatrix}, \tag{A11}$$

in which the diagonal Γ_t operator is

$$\Gamma_t = U\Gamma_0 U^{-1} = \begin{pmatrix} 1 + x & 0 & 0 \\ 0 & 1 - x & 0 \\ 0 & 0 & \Gamma \end{pmatrix}, \tag{A12}$$

and the transformed interaction potential is

$$V_t = UVU^{-1} = \frac{1}{\sqrt{2}p}\begin{pmatrix} 0 & 0 & p[\tilde{\Omega}_2(x + i\tilde{\Delta}) + p\tilde{\Omega}_1]/x \\ 0 & 0 & p[\tilde{\Omega}_2(x - i\tilde{\Delta}) - p\tilde{\Omega}_1]/x \\ \tilde{\Omega}_2 + \tilde{\Omega}_1(x - i\tilde{\Delta}) & \tilde{\Omega}_2 - \tilde{\Omega}_1(x + i\tilde{\Delta}) & 0 \end{pmatrix}. \tag{A13}$$

The equation of motion in terms of $V_\pm$ and C are then found to be

$$\frac{dV_+}{d\tau} = -(1 + x)V_+ - \frac{i}{\sqrt{2}x}[\tilde{\Omega}_2(x + i\tilde{\Delta}) + p\tilde{\Omega}_1]C, \tag{A14}$$

$$\frac{dV_-}{d\tau} = -(1 - x)V_- - \frac{i}{\sqrt{2}x}[\tilde{\Omega}_2(x - i\tilde{\Delta}) - p\tilde{\Omega}_1]C, \tag{A15}$$

$$\frac{dC}{d\tau} = -\tilde{\Gamma}C - \frac{i}{\sqrt{2}}[p\tilde{\Omega}_2 + \tilde{\Omega}_1(x - i\tilde{\Delta})]V_+ - \frac{i}{\sqrt{2}}[p\tilde{\Omega}_2 - \tilde{\Omega}_1(x + i\tilde{\Delta})]V_-, \tag{A16}$$

APPENDIX B: DERIVATION OF EMISSION AND ABSORPTION PROBABILITIES IN DRESSED BASIS

We start with amplitude equations in dressed basis (A14)–(A16). The initial conditions corresponding to the emission from the state C are $V_\pm(0) = 0$, $C(0) = 1$. Assuming the driving fields to be weak ($\tilde{\Omega}_{1,2} << 1$ we can solve Eqs. (A14)–(A16) by expansion in perturbation series over $\tilde{\Omega}_{1,2}$. The lowest order solution for $B(\tau)$ of Eq. (A16) yields $C^{(0)}(\tau) = e^{-\tilde{\Gamma}\tau}$. The latter can be substituted in Eqs. (A14) and (A15) to find $V_\pm^{(0)}(\tau)$:

$$V_\pm^{(0)}(\tau) = -i\frac{\tilde{\Omega}_2(x \pm i\tilde{\Delta}) \pm p\tilde{\Omega}_1}{\sqrt{2}x(1 \pm x - \tilde{\Gamma})}(e^{-\tilde{\Gamma}\tau} - e^{-(1\pm x)\tau}). \tag{B1}$$

The exponential approximation or $C(\tau)$ gives relatively good agreement with numerical simulations only for small time.

For large time the behavior of the system is far from being exponential. Therefore, we should consider next-order correction for $C(\tau)$. It can be done by substituting functions $V_{\pm}^{(0)}$ from Eq. (B1) to Eq. (A16) which yields

$$C^{(1)}(\tau) = \left[\frac{A_+}{1+x-\tilde{\Gamma}} + \frac{A_-}{1-x-\tilde{\Gamma}} - (A_+ + A_-)\tau\right] e^{-\tilde{\Gamma}\tau} + e^{-\tilde{\Gamma}\tau} - \frac{A_+}{1+x-\tilde{\Gamma}} e^{-(1+x)\tau} - \frac{A_-}{1-x-\tilde{\Gamma}} e^{-(1-x)\tau}, \tag{B2}$$

where

$$A_\pm = \frac{[p\tilde{\Omega}_2 \pm (x \mp i\tilde{\Delta})\tilde{\Omega}_1][\tilde{\Omega}_2(x \pm i\tilde{\Delta}) \pm p\tilde{\Omega}_1]}{2px(1 \pm x - \tilde{\Gamma})}. \tag{B3}$$

Using the definition for emission probability from Eq. (5) at large time $\tau \gg 1, 1/\tilde{\Gamma}$, neglecting higher order terms in $\tilde{\Omega}_{1,2}$ the probability of absorption yields

$$P_{\text{emiss}}(\infty|b) = \frac{(\tilde{\Gamma}+1)(|\tilde{\Omega}_1|^2 + |\tilde{\Omega}_2|^2) - 2p\tilde{\Omega}_1\tilde{\Omega}_2}{\tilde{\Gamma}[\tilde{\Delta}^2 + (\tilde{\Gamma}+1)^2 - p^2]}. \tag{B4}$$

Similarly one can derive the probability of absorption. We start from absorption from level v_1. The initial conditions for the system with population on v_1 in dressed states are $V_\pm(0) = \pm p/\sqrt{2}x$, $C(0) = 0$ [see Eq. (A10)]. In lowest order of $\tilde{\Omega}_{1,2}$, Eqs. (A14) and (A15) yield

$$V_{\pm}^{(0)}(\tau|v_1) = \pm\frac{p}{\sqrt{2}x} e^{-(1\pm x)\tau}. \tag{B5}$$

The corresponding zero-order solution of $C^{(0)}(\tau)$ of Eq. (A16) is given by

$$C^{(0)}(\tau|v_1) = B_+ e^{-(1+x)\tau} - B_- e^{-(1-x)\tau} + (B_- - B_+)e^{-\tilde{\Gamma}\tau}, \tag{B6}$$

where

$$B_\pm = i\frac{p\tilde{\Omega}_2 \pm \tilde{\Omega}_1(x \mp i\tilde{\Delta})}{2x(1 \pm x - \tilde{\Gamma})}. \tag{B7}$$

Therefore, probability of absorption from level v_1 for large time $\tau \gg 1, 1/\tilde{\Gamma}$ given by Eq. (7) reads

$$P_{\text{abs}}(\infty|v_1) = \frac{(\tilde{\Gamma}+2)|\tilde{\Omega}_1 - p\tilde{\Omega}_2|^2 + [\tilde{\Gamma}(1-p^2) + 2\tilde{\Delta}^2(\tilde{\Gamma}+1)]|\tilde{\Omega_1}|^2}{2(1+\tilde{\Delta}^2 - p^2)[\tilde{\Delta}^2 + (\tilde{\Gamma}+1)^2 - p^2]}. \tag{B8}$$

The probability of absorption from level v_2 can be derived in the same way as for level v_1. In this case, the initial conditions according to Eq. (A10) read $V_\pm(0) = (x \pm i\tilde{\Delta})/\sqrt{2}x$, $C(0) = 0$. In the lowest order of $\tilde{\Omega}_{1,2}$, Eqs. (A14) and (A15) have the following solution:

$$V_{\pm}^{(0)}(\tau|a_2) = \frac{x \pm i\tilde{\Delta}}{\sqrt{2}x} e^{-(1\pm x)\tau}. \tag{B9}$$

The corresponding zero-order solution of $C^{(0)}(\tau)$ of Eq. (A16) yields

$$C^{(0)}(\tau|v_1) = D_+ e^{-(1+x)\tau} + D_- e^{-(1-x)\tau} + (D_+ + D_-)e^{-\tilde{\Gamma}\tau}, \tag{B10}$$

where

$$D_\pm = i\frac{[p\tilde{\Omega}_2 \pm \tilde{\Omega}_1(x \mp i\tilde{\Delta})](x \pm i\tilde{\Delta})}{2px(1 \pm x - \tilde{\Gamma})}. \tag{B11}$$

Therefore, probability of absorption from level v_2 for $\tau \gg 1, 1/\tilde{\Gamma}$ given by Eq. (7) yields

$$P_{\text{abs}}(\infty|v_2) = \frac{(\tilde{\Gamma}+2)|\tilde{\Omega}_2 - p\tilde{\Omega}_1|^2 + [\tilde{\Gamma}(1-p^2) + 2\tilde{\Delta}^2(\tilde{\Gamma}+1)]|\tilde{\Omega_2}|^2}{2(1+\tilde{\Delta}^2 - p^2)[\tilde{\Delta}^2 + (\tilde{\Gamma}+1)^2 - p^2]}, \tag{B12}$$

which becomes Eq. (B8) if $\tilde{\Omega}_1 \leftrightarrow \tilde{\Omega}_2$.

[1] M. O. Scully and M. S. Zubairy, *Quantum Optics* (Cambridge Press, London, 1997).
[2] Z. Ficek and S. Swain, *Quantum Interference and Coherence* (Springer, New York, 2007).
[3] A. Ishizaki and G. Fleming, PNAS **106**, 17255 (2009).
[4] U. Fano, Phys. Rev. **124**, 1866 (1961).
[5] G. S. Agarwal, *Springer Tracts in Modern Physics: Quantum Optics* (Springer-Verlag, Berlin, 1974).
[6] S. E. Harris, Phys. Rev. Lett. **62**, 1033 (1989).
[7] M. O. Scully, S.-Y. Zhu, and A. Gavrielides, Phys. Rev. Lett. **62**, 2813 (1989).
[8] O. Kocharovskaya, Phys. Rep. **219**, 175 (1992).
[9] P. Mandel and O. Kocharovskaya, Phys. Rev. A **45**, 2700 (1992).
[10] E. S. Fry, X. Li, D. Nikonov, G. G. Padmabandu, M. O. Scully, A. V. Smith, F. K. Tittel, C. Wang, S. R. Wilkinson, and S. Y. Zhu, Phys. Rev. Lett. **70**, 3235 (1993).
[11] A. S. Zibrov, M. D. Lukin, D. E. Nikonov, L. Hollberg, M. O. Scully, V. L. Velichansky, and H. G. Robinson, Phys. Rev. Lett. **75**, 1499 (1995).
[12] G. G. Padmabandu, G. R. Welch, I. N. Shubin, E. S. Fry, D. E. Nikonov, M. D. Lukin, and M. O. Scully, Phys. Rev. Lett. **76**, 2053 (1996).
[13] A. K. Wojcik, F. Xie, V. R. Chaganti, A. A. Belyanin, and J. Kono, J. Mod. Opt. **55**, 3305 (2008).
[14] P. Vasinajindakaw, J. Vaillancourt, G. Gu, R. Liu, Y. Ling, and X. Lu, App. Phys. Lett. **98**, 211111 (2011).
[15] J. Faist, F. Capasso, C. Sirtori, K. W. West, and L. N. Pfeiffer, Nature (London) **390**, 589 (1997).
[16] H. Schmidt, K. L. Campman, A. C. Gossard, and A. Imamoglu, Appl. Phys. Lett. **70**, 3455 (1997).
[17] A. E. Miroshnichenko, S. Flach, and Y. S. Kivshar, Rev. Mod. Phys. **82**, 2257 (2010).
[18] H. M. Gibbs, G. Khitrova, and S. W. Koch, Nat. Phot. **5**, 275 (2011).
[19] M. O. Scully, Phys. Rev. Lett. **104**, 207701 (2010).
[20] M. O. Scully, K. R. Chapin, K. E. Dorfman, M. B. Kim, and A. A. Svidzinsky, PNAS **108**, 15097 (2011).

[21] A. A. Svidzinsky, K. E. Dorfman, and M. O. Scully (unpublished).
[22] M. O. Scully, M. S. Zubairy, G. S. Agarwal, and H. Walther, Science **299**, 862 (2003).
[23] A. P. Kirk, Phys. Rev. Lett. **106**, 048703 (2011).
[24] M. O. Scully, Phys. Rev. Lett. **106**, 049801 (2011).
[25] K. R. Chapin, K. E. Dorfman, A. A. Svidzinsky, and M. O. Scully, e-print arXiv:1012.5321.
[26] Z. Wang, Ann. Phys. **326**, 340 (2011).
[27] A. Imamoglu and R. J. Ram, Opt. Lett. **19**, 1744 (1994).
[28] M. O. Scully, Laser Phys. **17**, 635 (2007).
[29] M. O. Scully, E. S. Fry, C. H. Raymond Ooi, and K. Wodkiewicz, Phys. Rev. Lett. **96**, 010501 (2006).
[30] S. Das, G. S. Agarwal, and M. O. Scully, Phys. Rev. Lett. **101**, 153601 (2008)
[31] H. R. Xia, C. Y. Ye, and S. Y. Zhu, Phys. Rev. Lett. **77**, 1032 (1996).
[32] M. O. Scully, in *Coherent Control, Fano Interference, and Non-Hermitian Interactions, Workshop, May, 1999* (Kluwer Academic Publishers, Norwell, 2001).
[33] A. Sitek and P. Machnikowski, Phys. Status. Solidi B **248**, 847 (2011).
[34] P. K. Jha, Y. V. Rostovtsev, H. Li, V. A. Sautenkov, and M. O. Scully, Phys. Rev. A **83**, 033404 (2011)
[35] P. K. Jha, H. Li, V. A. Sautenkov, Y. V. Rostovtsev, and M. O. Scully, Opt. Commun. **284**, 2538 (2011).